Supplemental Material can be found at:
http://www.jbc.org/content/suppl/2011/11/28/M111.309849.DC1.html

THE JOURNAL OF BIOLOGICAL CHEMISTRY VOL. 287, NO. 2, pp. 1361–1370, January 6, 2012
Published in the U.S.A.

Early Alterations of Brain Cellular Energy Homeostasis in Huntington Disease Models*[S]

Received for publication, October 2, 2011, and in revised form, November 21, 2011 Published, JBC Papers in Press, November 28, 2011, DOI 10.1074/jbc.M111.309849

Fanny Mochel[‡§¶1], Brandon Durant[¶], Xingli Meng[¶], James O'Callaghan[‖], Hua Yu[**], Emmanuel Brouillet[‡‡], Vanessa C. Wheeler[§§], Sandrine Humbert[**], Raphael Schiffmann[**], and Alexandra Durr[‡]

*From [‡]INSERM UMR S975 and Assistance-Publique des Hôpitaux de Paris, Department of Genetics, Hôpital La Salpêtrière, 75013 Paris, France, the [§]University Pierre and Marie Curie, 75005 Paris, France, the [¶]Institute of Metabolic Disease, Baylor Research Institute, Dallas, Texas 75226, the [‖]Health Effects Laboratory Division, National Institute for Occupational Safety and Health, Centers for Disease Control and Prevention, Morgantown, West Virginia 26505, the **Institut Curie, CNRS UMR3306, INSERM U1005, 91405 Orsay, France, [‡‡]URA CEA-CNRS 2210, Service MIRCen, CEA, 92265 Fontenay-aux-Roses, France, and the [§§]Center for Human Genetic Research, Massachusetts General Hospital, Boston, Massachusetts 02114*

Background: We hypothesized cerebral energy deficit in Huntington disease (HD).
Results: We found increased brain phosphocreatine and creatine in two HD mouse models, preceding ATP decrease and motor symptoms.
Conclusion: We demonstrated chronic and early alterations in energy homeostasis associated with reduced phosphocreatine utilization in HD.
Significance: These findings suggest that energy deficit is a relevant therapeutic target in HD.

Brain energy deficit has been a suggested cause of Huntington disease (HD), but ATP depletion has not reliably been shown in preclinical models, possibly because of the immediate post-mortem changes in cellular energy metabolism. To examine a potential role of a low energy state in HD, we measured, for the first time in a neurodegenerative model, brain levels of high energy phosphates using microwave fixation, which instantaneously inactivates brain enzymatic activities and preserves *in vivo* levels of analytes. We studied HD transgenic R6/2 mice at ages 4, 8, and 12 weeks. We found significantly increased creatine and phosphocreatine, present as early as 4 weeks for phosphocreatine, preceding motor system deficits and decreased ATP levels in striatum, hippocampus, and frontal cortex of R6/2 mice. ATP and phosphocreatine concentrations were inversely correlated with the number of CAG repeats. Conversely, in mice injected with 3-nitroproprionic acid, an acute model of brain energy deficit, both ATP and phosphocreatine were significantly reduced. Increased creatine and phosphocreatine in R6/2 mice was associated with decreased guanidinoacetate *N*-methyltransferase and creatine kinase, both at the protein and RNA levels, and increased phosphorylated AMP-dependent protein kinase (pAMPK) over AMPK ratio. In addition, in 4-month-old knock-in $Hdh^{Q111/+}$ mice, the earliest metabolic alterations consisted of increased phosphocreatine in the frontal cortex and increased the pAMPK/AMPK ratio. Altogether, this study provides the first direct evidence of chronic alteration in homeostasis of high energy phosphates in HD models in the earliest stages of the disease, indicating possible reduced utilization of the brain phosphocreatine pool.

Huntington disease (HD)[2] is inherited as an autosomal dominant trait and is characterized by diverse motor, cognitive, and psychiatric abnormalities. An expansion of 36 or more CAG repeats in the coding sequence of the *Huntingtin* (*HTT*) gene encoding the protein huntingtin has been identified as the genetic cause of this disorder (1, 2). Presymptomatic testing allows at risk persons to access their genetic status and thus predict that a carrier will go on to develop HD before showing clinical symptoms and signs. Having access to a presymptomatic population provides a unique possibility of approaching early physiopathological changes in HD.

Brain hypometabolism predominating in the basal ganglia has been suggested in the etiology of HD, because reduced glucose consumption starts in the presymptomatic stages of the disease (3). Various mechanisms may underlie the early energy deficit in HD brain (4) including impaired oxidative phosphorylation (5), decreased glycolysis (6), and/or transcriptional deregulation of key factors of mitochondrial metabolism such as the transcriptional coactivator peroxisome proliferator-activated receptor coactivator-1α (7). In addition, the inhibition of succinate dehydrogenase by 3-nitropropionic acid, or malonate, mimics HD neuropathology in rats, mice, and nonhuman primates (8, 9). However, ATP depletion in HD brain has not been demonstrated. Immediate post-mortem changes in brain enzymatic activities account for the technical difficulties of reliably measuring ATP concentrations in preclinical models. Likewise, ATP levels are known to decrease dramatically within seconds of interruption of blood supply to the brain (10). This post-mortem effect can be prevented by the use of microwave radiation provided by a microwave fixation system (11). This system instantly inactivates brain enzymes and conserves con-

* This work was supported, in whole or in part, by National Institutes of Health Grants NS32765 and NS049206 (to V. C. W.). This work was also supported by the CHDI Foundation, Inc.
[S] This article contains supplemental Fig. S1.
[1] To whom correspondence should be addressed: Brain and Spine Institute, INSERM UMR S975, Hôpital de La Salpêtrière, 75013 Paris, France. Tel.: 33-1-57-27-46-82; E-mail: fanny.mochel@upmc.fr.

[2] The abbreviations used are: HD, Huntington disease; AMPK, AMP-dependent protein kinase; pAMPK, phospho-AMPK; 3NP, 3-nitropropionic acid; BB-CK, brain isoform of creatine kinase; AGAT, glycine amidinotransferase; GAMT, guanidinoacetate *N*-methyltransferase.

Downloaded from www.jbc.org at CDC Information Center, on February 10, 2012

centrations of adenine nucleotides while preserving the structure of the brain for regional dissection. Probably because of limited access to this technique, there are almost no data available in the literature on energy metabolite levels in rodent brain. To our knowledge, one single study reliably reported AMP, ADP, and ATP values in different cerebral regions (12), but such a study was performed in WT rats and not in mice. Moreover, the technique was never validated in a disease model in which a brain energy deficit was suspected.

Here, we directly tested the hypothesis that brain energy deficit exists in HD and that it correlates with the core characteristics of disease. We studied the R6/2 *HTT* exon 1 transgenic HD murine model, known to exhibit metabolic abnormalities (13, 14) including hypercatabolism (15) as seen in HD patients at the earliest stages of the disease (16), as well as knock-in $Hdh^{Q111/+}$ heterozygous mice in which an expanded CAG repeat is inserted into one allele of the mouse *HTT* homologue gene (17).

EXPERIMENTAL PROCEDURES

Mouse Colonies and Behavioral Studies—All of the animals were handled in strict accordance with good animal practice as defined by the Texas animal welfare bodies, and all of the animal work was approved by the institutional animal care and use committee at the Baylor Research Institute (Dallas, TX; 007_001). 4-, 8-, and 12-week-old transgenic R6/2 mice and WT littermates obtained from Jackson Laboratory (Bar Harbor, ME) were maintained on a 12-h light/12-h dark, temperature-controlled environment. The mice were given *ad libitum* access to food and water. At 3 weeks of age, tail snips were obtained and sent to Laragen Inc. (Los Angeles, CA) for genotyping and sequencing of CAG repeats. The mice were housed three to five per cage in an enriched environment as used by PsychoGenics (best practices protocol). Body weight was monitored weekly throughout the experiments. Behavioral studies included grip test and high resolution behavior analyses using a home cage video tracking system.

Grip Test—The mice were placed on the grip strength apparatus in such a way that the animals grabbed a small triangular handle with its forepaws and then were slowly pulled away from the handle by the tail until they released the handle. The equipment automatically measured the strength of the animal's grip in grams. Five scores were recorded per animal in consecutive sequence, and means for the tension peak (gf), *i.e.* the force applied to the bar at the moment the grasp is released, were calculated for each animal based on the four best scores. The testing with the grip test was performed on R6/2 and WT mice at 5 and 8 weeks of age.

Home Cage—Four digital video cameras were mounted perpendicular to the cages. Video data were analyzed by HomeCageScan software (Clever Systems, Reston, VA). During recording, the mice were housed in polycarbonate cages (Lab Product, Seaford, DE) to improve the video tracking of the mice, with minimal bedding (80 ml) to minimize mounding, which can obscure the mouse. Each mouse was recorded individually for 24 h, with 12 h of daylight and 12 h of dim red light. Feeding behaviors such as eating and drinking were detected when the mouth of the animal touched the respective calibrated landmark on the cage (food bin and water spout) for a given minimum length of time and were expressed as bouts, *i.e.* occurrence of a single eating behavior. Hanging behaviors were detected when the animal was suspended from the cage top and were expressed as percentages of time. We recorded R6/2 and WT mice at 4, 8, and 12 weeks of age.

In addition, congenic C57BL/6J Hdh^{Q111} mice and their WT littermates obtained from the lab of Vanessa Wheeler were generated as described (18) and maintained by crossing to WT C57BL/6J mice from the Jackson Laboratories. Mouse genotyping and CAG repeat length determination were performed as described previously (19).

Collection of Brain Samples after Microwave Fixation—If not stated otherwise, all of the mice from the study were killed by focused microwave irradiation using a 10 kW Muromachi Microwave Applicator, Model TMW-4012C (Stoelting Co., Wood Dale, IL), as detailed (20). The Muromachi system has a specially designed applicator unit that radiates a microwave beam focused on the head of a rat or mouse, resulting in death within $<$50 ms and elevations of brain temperature to 90 °C within 1 s (mouse). In addition, the use of a water jacket surrounding the animal holder allows a homogenous distribution of the irradiation throughout the whole brain. Water in the holder jacket becomes hot after irradiation and therefore was replaced with new water for each sacrifice. Exposure time, power, and position of the holder in the applicator unit were adjusted according to previously determined settings appropriate for each weight/age group. Regional brain dissection was performed on ice to isolate striatum, hippocampus, and frontal cortex. Following dissection, the samples were immediately placed on dry ice and then kept frozen at −80 °C until tissue assay.

In a subset of 10 weeks old B6CBA WT mice, 3-nitropropionic acid (3NP) was injected intraperitoneally at the dose of 180 mg/kg. The mice were then sacrificed using the Muromachi microwave system 1 h after the 3NP injection.

Measurement of Brain High Energy Phosphates and Creatine by HPLC—To further improve the sensitivity of the high energy phosphates analysis, we implemented a new method derived from Williams *et al.* (21), allowing us to (i) improve the accuracy of our measurements for AMP, ADP, and ATP by neutralizing the extracted samples, as well as to (ii) simultaneously detect creatine and phosphocreatine, which are very sensitive markers of cellular energy status. A Waters HPLC system was equipped with an ESA model 580 solvent delivery module, a Shimadzu SPD-10A UV-visible detector, and a Shimadzu integrator. Separations were done on a YMC-Pack Pro C18 reversed phase column (0.46 × 25 cm I.D., S - 3 μm, 12 nm) with an injection volume of 5 μl. The mobile phase consisted of a gradient using two buffers. The first buffer (A) contained 0.1 M KH_2PO_4, 5 mM tetrabutylammonium hydrogen sulfate, and 2.5% (v/v) acetonitrile (pH 5.85). The second buffer (B) contained 0.1 M KH_2PO_4, 5 mM tetrabutylammonium hydrogen sulfate, and 25% (v/v) acetonitrile (pH 5.5). The column was eluted for 3 min with buffer A, for 2 min with buffers A and B (steadily increasing to 11%), and for 25 min with a steady increase to 100% buffer B. The column was re-equilibrated for 15 min with 100% buffer A. Flow was maintained at 1.0 ml/min,

Downloaded from www.jbc.org at CDC Information Center, on February 10, 2012

and separations were done at 50 °C. Detection of AMP, ADP, and ATP was done at 260 nm, and detection of creatine and phosphocreatine was performed at 220 nm. The peaks were identified using coelution with standards and were quantified against a standard curve. The retention times were: creatine, 3.1 min; phosphocreatine, 5.0 min; AMP, 9.7 min; ADP, 16.4 min; and ATP, 22.4 min. The samples were deproteinized using a 0.4 M perchloric acid solution containing dithioerythritol (1 mg/ml) and diethylenetriaminepent aacetic acid (0.1 mg/ml), homogenized (Wheaton homogenizer), and centrifuged for 20 min at +4 °C at top speed (13.8–14.5 rpm). The supernatant (30 μl) was neutralized with 3.8 μl of 2 M Na2CO3 (1:8 Na_2CO_3: perchloric acid, adapted from Matthews *et al.* (47). Two standards were used: a 2 mM PCr/Creatine standard was prepared fresh for each run both deprotonized and neutralized, and a 250 μM AMP/ADP/ATP standard was prepared from stock 1 mM solutions (−80 °C) diluted with 0.4 M perchloric acid and neutralized (2 M Na_2CO_3).

Western Blots—Immunoblot analyses were performed in both microwaved brain samples and brain samples obtained from mice after decapitation. Primary antibodies used in this study were AMP-dependent protein kinase (AMPK) (AMPkα, sc2532), phospho-AMPK (pAMPkα, sc2535) (Santa Cruz Biotechnology, Santa Cruz, CA), the brain isoform of creatine kinase (BB-CK, AB38211) (Abcam, Cambridge, MA), glycine amidinotransferase (AGAT), and guanidinoacetate *N*-methyltransferase (GAMT) synthesized by Wallimann/Braissant (22).

Microwaved brain regions were homogenized in 10 volumes of hot (85–95 °C) 1% SDS. Total protein was determined by bicinchoninic acid method (23) using bovine serum albumin as standard. Phospho-specific or pan-specific antibodies were directed against specific phospho-sites or specific proteins, and quantification was achieved with detection of fluorescent signals using an infrared fluorescence scanner (Licor Biosciences, Lincoln, NE). Following incubation with primary antibodies, the blots were washed with phosphate-buffered saline with 0.1% Tween 20 (1 × 15 min; 2 × 5 min) and incubated with fluorescent-labeled anti-rabbit and anti-mouse IgG antibodies (1:2500) for 1 h.

The same experiments were performed on brain samples from R6/2 and $HdhQ^{Q111}$ mice at 8 weeks and 4 months of age, respectively, obtained after decapitation. The frontal cortex and striatum of the brains were rapidly removed on ice and were rapidly frozen in liquid nitrogen. The tissues were homogenized in lysis buffer consisted of 50 mM Tris-HCl, pH 7.5, 150 mM NaCl, 1% Triton, 2 mM EDTA, 2 mM EGTA, 1/100 protease inhibitor mixture (Sigma P8340), 1 mM PMSF (Sigma, P7626), and 1/200 phosphatase inhibitor mixture (Sigma, P5726). The lysates were centrifuged at 10,000 × g for 10 min at 4 °C. The supernatant was collected. Equal amounts of protein (30 μg) were electrophoresed under reducing conditions on 8 and 12% polyacrylamide gels transferred to nitrocellulose membrane (Bio-Rad). The immunodetection buffer used was Tris-buffered saline (10 mM Tris-HCl, 200 mM NaCl, and 0.1% Tween 20, pH 7.4). Nonspecific binding was saturated by incubation with 5% nonfat dried milk/Tris-buffered saline for 1 h. The blots were incubated overnight at 4 °C with primary antibodies.

Quantitative PCR mRNA Analyses—Total RNA was isolated from nonmicrowaved brain samples using miRNeasy mini kit (Qiagen). After treatment with DNase I (Invitrogen), reverse transcription was performed using SuperScript II with 1 μg of RNA and random hexamers (Invitrogen). Quantitative PCR was performed using an ABI StepOnePlus real time PCR system with predesigned TaqMan probe and primers for mouse BB-CK, AGAT, GAMT, the brain creatine transporter SLC6A8, and AMPK that were purchased from Applied Biosystems (ABI, Foster City, CA). 18 S rRNA was used as internal control and detected by TaqMan probe and primers (ABI).

Statistics—For comparison of means and correlations, parametric (analysis of variance and Pearson) or nonparametric tests (Spearman) were used as appropriate (SPSS, Chicago, IL). To analyze the relationship between the number of CAG repeats and the levels of brain metabolites, we used a multiple linear regression analysis with age as a covariate and restricted maximum likelihood estimation.

RESULTS

Locomotor Deficit and Hypercatabolism in 8- and 12-week-old R6/2 Mice—The number of CAG repeats influences R6/2 mouse phenotypes (24). Therefore, we first characterized motor and metabolic abnormalities of our R6/2 colony. The number of CAG repeats obtained from tail genotyping in R6/2 mice ranged from 100 to 126. The parameters were analyzed separately for male and female because body weight is a confounding factor for locomotor testing. Ten to fifteen mice were used per genotype per sex.

The grip test performed at 8 weeks of age showed a significant decrease of grip strength in both R6/2 male (128 ± 15 gf *versus* 178 ± 23 gf, $p < 0.001$) and female (116 ± 16 gf *versus* 149 ± 13 gf, $p < 0.001$) compared with WT littermates. The number of CAG repeats was inversely correlated with the grip strength at 8 weeks ($r = -0.443$, $p = 0.018$). However, no difference was detected between genotypes at 4 weeks of age (153 ± 19 gf *versus* 152 ± 30 gf, for males; 121 ± 13 gf *versus* 131 ± 20 gf, for females). Because handling-induced anxiety complicates interpretation of behavioral data, especially in models like the R6/2 mice that are prone to seizures when stressed, we chose a testing paradigm in a home cage environment that could provide relevant information on the locomotor phenotype with fewer confounding factors that other assessment options. Likewise, we found a significant decrease of total time spent hanging in 8- and 12-week-old R6/2 males (4.3 ± 3.7% *versus* 7.7 ± 3.0, $p = 0.031$; and 1.4 ± 1.6% *versus* 5.2 ± 3.5, $p < 0.001$) and females (6.4 ± 3.0% *versus* 8.6 ± 3.0, $p = 0.030$; and 1.8 ± 2.3% *versus* 6.8 ± 1.8, $p < 0.001$). The number of CAG repeats was negatively correlated with hanging in 12-week-old R6/2 mice ($r = -0.606$, $p = 0.001$). However, we did not observe any change in locomotor phenotype in HD mice at 4 weeks of age, *e.g.* total time spent hanging (5.4 ± 2.8% *versus* 4.8 ± 1.9 for males; 7.8 ± 3.6% *versus* 8.0 ± 2.8 for females), confirming that the mice did not exhibit overt motor deficits at this age.

Body weight, monitored weekly, also was affected in R6/2 mice. A progressive decrease in growth of R6/2 mice started around 10 weeks of age. We observed a lower body weight at 12

Downloaded from www.jbc.org at CDC Information Center, on February 10, 2012

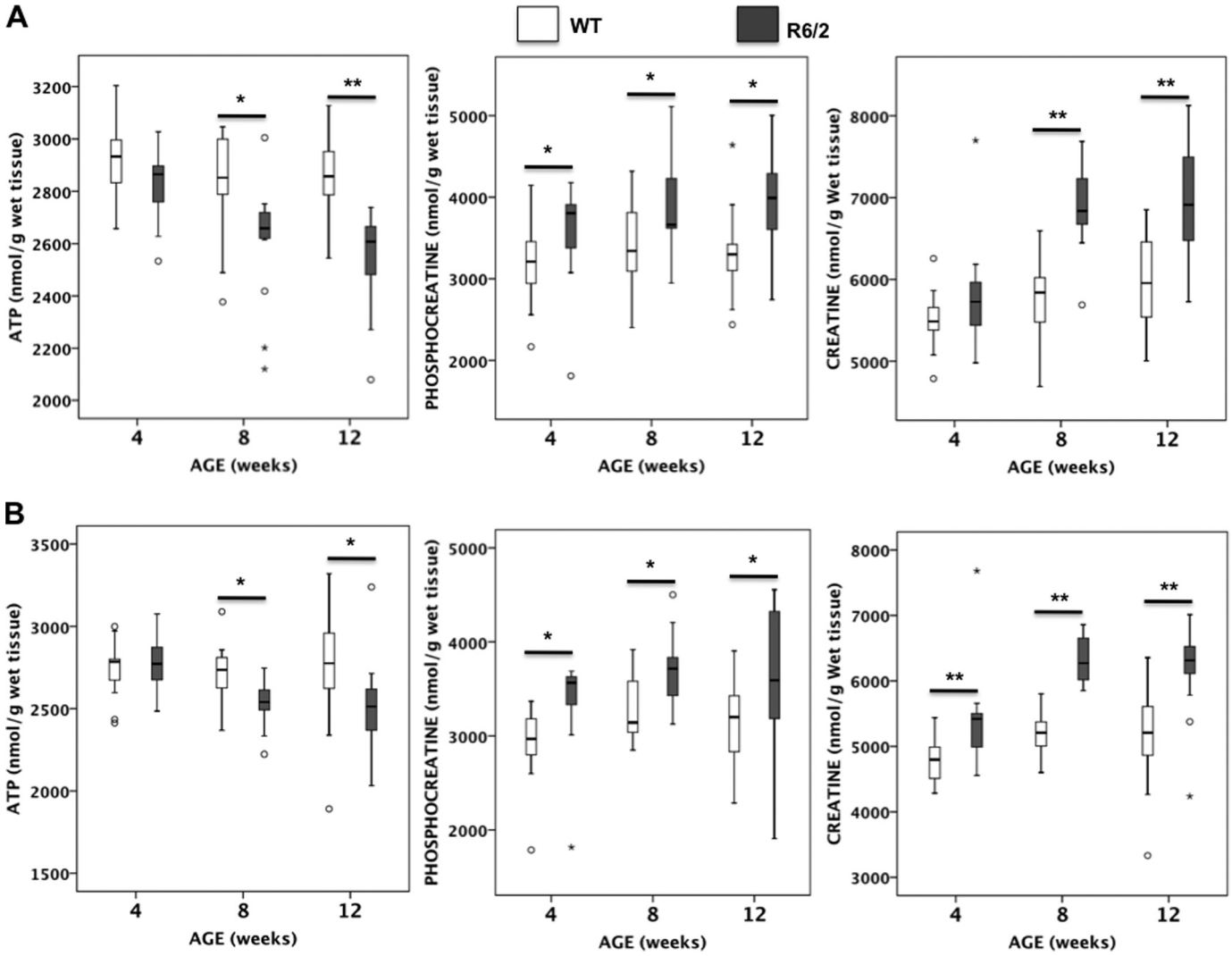

FIGURE 1. **Brain energy metabolites in R6/2 and WT mice after microwave irradiation.** ATP, phosphocreatine, and creatine levels were measured by HPLC in striatum and frontal cortex of R6/2 and WT mice at 4, 8, and 12 weeks of age; the number of animals was 16 ± 2 per group as indicated in Table 1. The box plots show the medians and the interquartile ranges, *i.e.* the difference between the 75th and 25th percentiles. The *circles* and *stars* denote outliers that are farther than 1.5 and 3 interquartile ranges, respectively, from the nearer edge of the box. *, $p < 0.05$; **, $p < 0.001$.

weeks in both R6/2 males (24.5 ± 2.2 g *versus* 35.1 ± 2.3 g, $p < 0.001$) and females (22.7 ± 3.1 g *versus* 26.5 ± 4.4 g, $p = 0.058$) compared with WT. This was associated with significantly increased eating behaviors, as detected by the HomeCageScan analyses, at 12 weeks for both R6/2 male (4736 ± 2020 bouts *versus* 1991 ± 496 bouts, $p < 0.001$) and female mice (4291 ± 1649 bouts *versus* 1756 ± 449 bouts, $p < 0.001$). Of note, despite a lack of a difference in body weight at 8 weeks of age, R6/2 males and females showed a significantly increased food intake (3511 ± 1033 bouts *versus* 2051 ± 998 bouts, $p = 0.003$, for males; 2259 ± 671 bouts *versus* 1807 ± 490 bouts, $p = 0.025$, for females). Therefore, increased feeding behaviors prior to overt changes in body weight suggested hypercatabolism in R6/2 mice. At 12 weeks, the number of CAG repeats correlated with eating-related behaviors ($r = 0.509$, $p = 0.006$).

Identification of a Chronic Brain Energy Deficit in R6/2 Mice—Compared with WT littermates, we found a significant decrease of ATP in the striatum (−11%), hippocampus (−9%), and frontal cortex (−9%) of 12-week-old R6/2 mice (Fig. 1). A significant decrease of ATP was also measured in the three brain regions (−9%, −8%, and −6%, respectively) of R6/2 mice at 8 weeks of age, but no difference was found compared with WT in presymptomatic 4-week-old R6/2 mice (Fig. 1). Unexpectedly, R6/2 mice also displayed significantly increased phosphocreatine in the striatum (+13%) and frontal cortex (+13%) at 8 weeks of age and in the striatum (+19%) and hippocampus (+12%) at 12 weeks of age, together with a significant increase in the phosphocreatine to ATP ratio in these regions (Fig. 1 and Table 1). This was associated with a significant increase in creatine levels in cortex, hippocampus, and frontal cortex of R6/2 mice at 8 weeks (+19%, +12%, and +22%, respectively) and 12 weeks (+15%, +10%, and +21%, respectively) compared with WT mice (Fig. 1). Despite normal ATP levels at 4 weeks of age, phosphocreatine was significantly increased in both striatum (+15%) and frontal cortex (+17%) of R6/2 mice, resulting in an increase in the phosphocreatine to ATP ratio (Table 1), associated with a significantly increased creatine level in frontal cortex (+12%) (Fig. 1). Therefore, the increased phosphocreatine

Downloaded from www.jbc.org at CDC Information Center, on February 10, 2012

TABLE 1
High energy phosphates profile measured by HPLC in brain of WT and R6/2 mice sacrificed by microwave fixation at 4, 8, and 12 weeks of age
NS, not significant.

Brain region	Genotype	Age	*n*	Creatine	PCr	AMP	ADP	ATP	ATP/AMP ratio	PCR/ATP ratio
		weeks		*nmol/g*	*nmol/g*	*nmol/g*	*nmol/g*	*nmol/g*		
Striatum	R6/2	4	14	5813 ± 634	3606 ± 609	95 ± 18	556 ± 35	2837 ± 141	30.7 ± 6.0	1.3 ± 0.2
	WT		15	5496 ± 344	3180 ± 468	87 ± 16	545 ± 50	2918 ± 134	34.6 ± 6.3	1.1 ± 0.1
	p value			NS	0.043	NS	NS	NS	NS	0.007
Hippocampus	R6/2	4	14	6298 ± 711	4080 ± 605	106 ± 30	560 ± 47	2735 ± 123	27.8 ± 7.5	1.5 ± 0.2
	WT		15	5903 ± 434	3884 ± 432	89 ± 16	533 ± 48	2720 ± 141	31.3 ± 5.5	1.4 ± 0.2
	p value			0.080	NS	0.077	NS	NS	NS	NS
Frontal cortex	R6/2	4	14	5412 ± 734	3365 ± 487	126 ± 29	605 ± 43	2773 ± 167	23.2 ± 5.3	1.2 ± 02
	WT		15	4763 ± 342	2920 ± 387	114 ± 37	572 ± 63	2740 ± 165	25.7 ± 6.2	1.1 ± 0.1
	p value			0.005	0.011	NS	NS	NS	NS	0.015
Striatum	R6/2	8	15	6888 ± 483	3850 ± 513	104 ± 16	541 ± 36	2615 ± 219	25.8 ± 4.4	1.5 ± 0,1
	WT		15	5786 ± 479	3410 ± 543	100 ± 24	569 ± 57	2826 ± 198	29.5 ± 6.0	1.2 ± 0.2
	p value			<0.001	0.031	NS	NS	0.010	0.064	<0.001
Hippocampus	R6/2	8	15	7060 ± 583	3943 ± 561	103 ± 36	530 ± 70	2498 ± 184	26.6 ± 7.7	1.6 ± 0.2
	WT		15	6313 ± 563	4030 ± 591	98 ± 27	561 ± 54.6	2723 ± 54.6	29.7 ± 7.1	1.5 ± 0.2
	p value			0.001	NS	NS	NS	0.003	NS	NS
Frontal cortex	R6/2	8	15	6330 ± 345	3695 ± 371	121 ± 25	583 ± 44	2533 ± 137	21.6 ± 3.9	1.5 ± 0.1
	WT		14	5180 ± 340	3283 ± 346	129 ± 45	623 ± 75	2708 ± 188	22.9 ± 6.7	1.2 ± 0.1
	p value			<0.001	0.005	NS	NS	0.008	NS	<0.001
Striatum	R6/2	12	18	6855 ± 670	3935 ± 609	91 ± 19	543 ± 54	2552 ± 169	29.4 ± 6.6	1.5 ± 0.2
	WT		18	5941 ± 525	3298 ± 485	85 ± 21	563 ± 49	2862 ± 136	35.2 ± 7.5	1.2 ± 0.2
	p value			<0.001	0.001	NS	NS	<0.001	0.019	<0.001
Hippocampus	R6/2	12	18	6879 ± 538	4081 ± 599	92 ± 20	539 ± 51	2522 ± 135	28.9 ± 7.5	1.6 ± 0.2
	WT		17	6266 ± 736	3645 ± 673	80 ± 19	541 ± 62	2766 ± 238	36.4 ± 9.2	1.3 ± 0.2
	p value			0.008	0.051	NS	NS	0.001	0.013	<0.001
Frontal cortex	R6/2	12	18	6205 ± 626	3571 ± 764	119 ± 25	586 ± 82	2508 ± 241	21.9 ± 4.3	1.4 ± 0.3
	WT		15	5121 ± 856	3148 ± 472	123 ± 39	625 ± 97	2767 ± 358	24.2 ± 6.0	1.1 ± 0.2
	p value			<0.001	0.072	NS	NS	0.019	NS	0.001

and/or creatine in 4-week-old R6/2 mice preceded the decrease in ATP and motor disease onset and was not restricted to the striatum. In addition, in striatum, hippocampus, and frontal cortex, we observed a systematic decrease in the ATP/AMP ratio in R6/2 mice compared with WT littermates, which reached significance at 12 weeks of age (Table 1).

Negative Correlation between the Number of CAG Repeats and High Energy Phosphates in the Striatum of R6/2 Mice—After adjusting for age, we found a negative association between the number of CAG repeats and ATP levels in the striatum of R6/2 mice ($p = 0.012$). For every one-unit increase of CAG, ATP decreased by 13.40 nmol/g. Therefore, we obtained the following estimated model: ATP = $-13.40 \times$ CAG + 4375.08 (if age 4 weeks), 4214.45 (if age 8 weeks), or 4080.95 (if age 12 weeks) (Fig. 2). In addition, after age correction, we found that the number of CAG repeats was negatively associated with phosphocreatine levels in the striatum of R6/2 mice ($p = 0.013$). For every one-unit increase of CAG, phosphocreatine decreased by 43.01 nmol/g. Likewise, the estimated model was: phosphocreatine = $-43.01 \times$ CAG + 8507.39 (if age 4 weeks) or 8984.79 (if age 8 weeks) or 8842.13 (if age 12 weeks) (Fig. 2). There was no correlation between the number of CAG repeats and the levels of high energy phosphates in the hippocampus or frontal cortex.

Acute Brain Energy Deficit in the 3NP Model—To compare the high energy phosphate profile that we observed in R6/2 mice, a model for chronic neurodegeneration, with an acute model of energy-related striatal neurodegeneration (9), we administered 3NP (180 mg/kg) to 10-week-old B6CBA WT mice. One hour following the 3NP injection, we observed a 9% decrease of ATP (Fig. 3) and ADP (506 ± 54 nmol/g *versus* 563 ± 49 nmol/g, $p = 0.016$) in the striatum compared with uninjected mice. This finding is consistent with the 10–20% decrease in striatal ATP concentrations reported after microwave fixation of mice injected with 1-methyl-4-phenyl-1,2,3,6-tetrahydropyridine (25). In contrast to what was seen in 10-week-old R6/2 mice (*i.e.* 10% decreased ATP and 16% increased phosphocreatine), 3NP injection also resulted in a 24% reduction of phosphocreatine (Fig. 3) and a corresponding reduction in the phosphocreatine to ATP ratio (0.98 ± 0.15 *versus* 1.15 ± 0.17, $p = 0.034$). No differences were measured in the levels of striatal creatine or high energy phosphate in the hippocampus or frontal cortex of 3NP-injected mice compared with WT mice. Therefore, in an acute model of energy deficit, a decrease in most high energy phosphate metabolites (ADP, ATP, and phosphocreatine) was observed in the striatum.

Potential Mechanisms Underlying Increased Creatine and Phosphocreatine in the Brain of R6/2 Mice—To understand the expanded cerebral pools of creatine and phosphocreatine in R6/2 mice, we analyzed the expression of the two creatine biosynthetic enzymes AGAT and GAMT, the brain creatine transporter SLC6A8, and BB-CK that regulates the balance between creatine and phosphocreatine in the brain.

First, we found no change in AGAT expression at the RNA or protein levels between R6/2 and WT mice (supplemental Fig. S1). However, GAMT expression was decreased both at the RNA ($p = 0.026$) and protein ($p = 0.001$) levels in the frontal cortex of 8-week-old R6/2 mice compared with WT littermates (supplemental Fig. S1). Second, we observed no significantly different expression of SLC6A8 mRNA between R6/2 and WT mice in the striatum (0.64 ± 0.22 relative units *versus* 5.0 ± 3.5 relative units) and in the frontal cortex (1.08 ± 0.09 relative units *versus* 1.07 ± 0.32 relative units). We were not able to assess SLC6A8 protein levels because of the lack of reliable antibodies. Finally, we found decreased mRNA expression of

Downloaded from www.jbc.org at CDC Information Center, on February 10, 2012

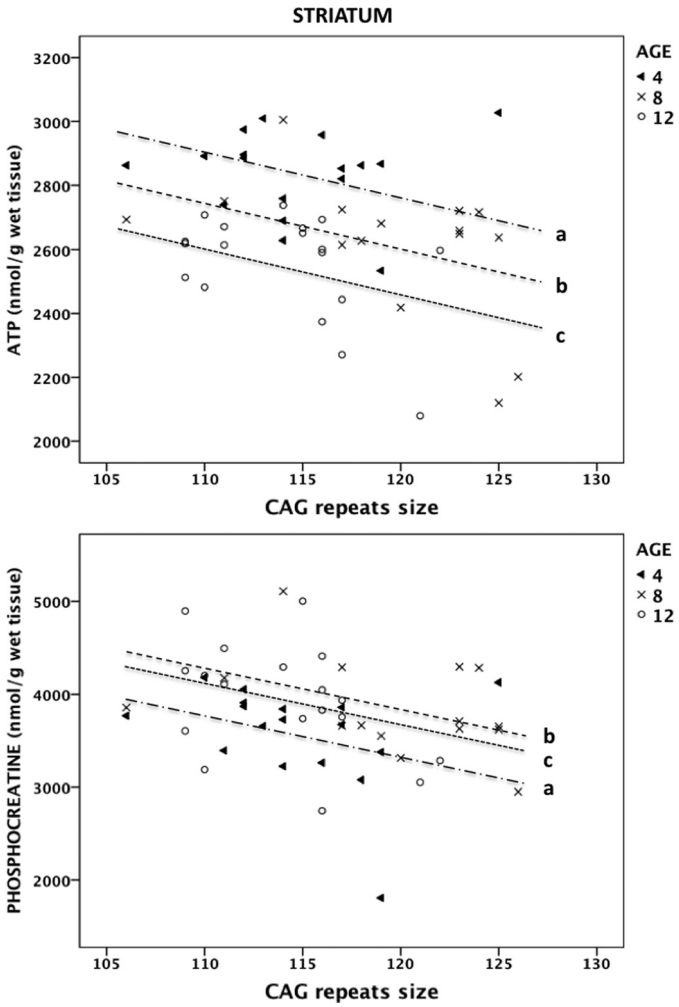

FIGURE 2. **Relationship between CAG repeats and striatal high energy phosphates in R6/2 mice.** The values of ATP (*upper panel*) and phosphocreatine (*lower panel*) are plotted against the number of CAG repeats. Using a multiple linear regression analysis with age as a covariate and restricted maximum likelihood estimation, *a*, *b*, and *c* correspond to the regression lines at 4, 8, and 12 weeks of age, respectively.

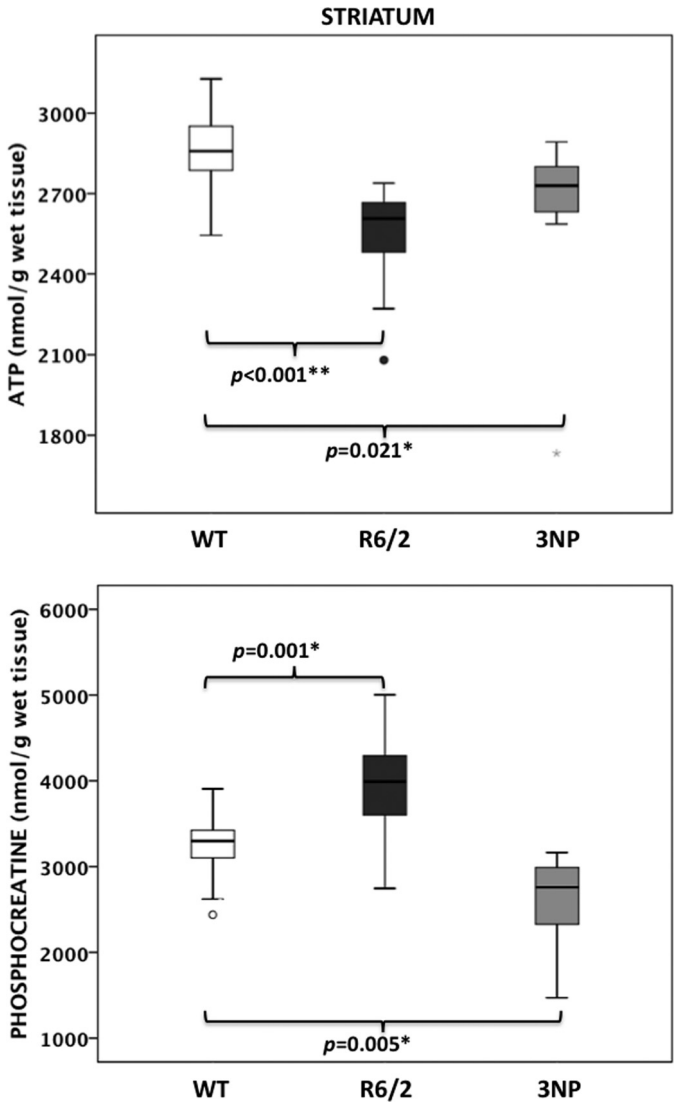

FIGURE 3. **Brain energy high energy phosphates in the acute 3NP model.** ATP and phosphocreatine levels were measured by HPLC in striatum of 10-week-old WT mice 1 h after 3NP injection and compared with age-matched WT and R6/2 mice; the number of animals was 12 ± 2 per group. The box plots show the medians and the interquartile ranges, *i.e.* the difference between the 75th and 25th percentiles. The *circles* and *stars* denote outliers that are farther than 1.5 and 3 interquartile ranges, respectively, from the nearer edge of the box. *, $p < 0.05$; **, $p < 0.001$.

BB-CK in the frontal cortex ($p = 0.039$) of R6/2 mice compared with WT littermates (supplemental Fig. S1). This was associated with decreased protein levels of BB-CK in the striatum ($p = 0.010$) and frontal cortex ($p = 0.006$) of 8-week-old microwaved R6/2 mice compared with WT littermates (supplemental Fig. S1). Of note, the decrease of BB-CK protein expression also was observed in nonmicrowaved brain samples. Altogether, these data indicated that the increased cellular pool of creatine and phosphocreatine in R6/2 brain was not explained by increased cerebral synthesis or transport of creatine into the brain.

Phosphocreatine Is Increased in the Brain of $Hdh^{Q111/+}$ Heterozygous Knock-in Mice—To assess the brain energy deficit that occurs in response to a single endogenous allele's worth of full-length mutant huntingtin, as occurs in the majority of HD patients, we assessed high energy phosphate levels in heterozygous $Hdh^{Q111/+}$ knock-in mice. Thirteen 4-month-old $Hdh^{Q111/+}$ mice, with CAG alleles ranging from 122 to 129, and 13 WT littermates were sacrificed by microwave fixation as described earlier. Compared with WT, we found increased phosphocreatine (3722 ± 330 nmol/g protein *versus* 3296 ± 636 nmol/g protein, $p = 0.043$) in the frontal cortex of $Hdh^{Q111/+}$ mice. In the striatum of $Hdh^{Q111/+}$ mice, there also was increased phosphocreatine (3528 ± 309 nmol/g protein *versus* 3236 ± 579 nmol/g protein), although this increase did not reach statistical significance. Of note, the small range of CAG repeat lengths in $Hdh^{Q111/+}$ mice did not allow testing the correlation with the levels of phosphocreatine. There was no change in creatine or adenine nucleotides in $Hdh^{Q111/+}$ mice compared with WT mice. In addition, we did not find any significant change in the RNA or protein levels of AGAT, GAMT, SLC6A8, and BB-CK in 4-month-old $Hdh^{Q111/+}$ mice compared with WT littermates. These data suggest that increased brain phosphocreatine occurs early in the HD pathogenic process.

Downloaded from www.jbc.org at CDC Information Center, on February 10, 2012

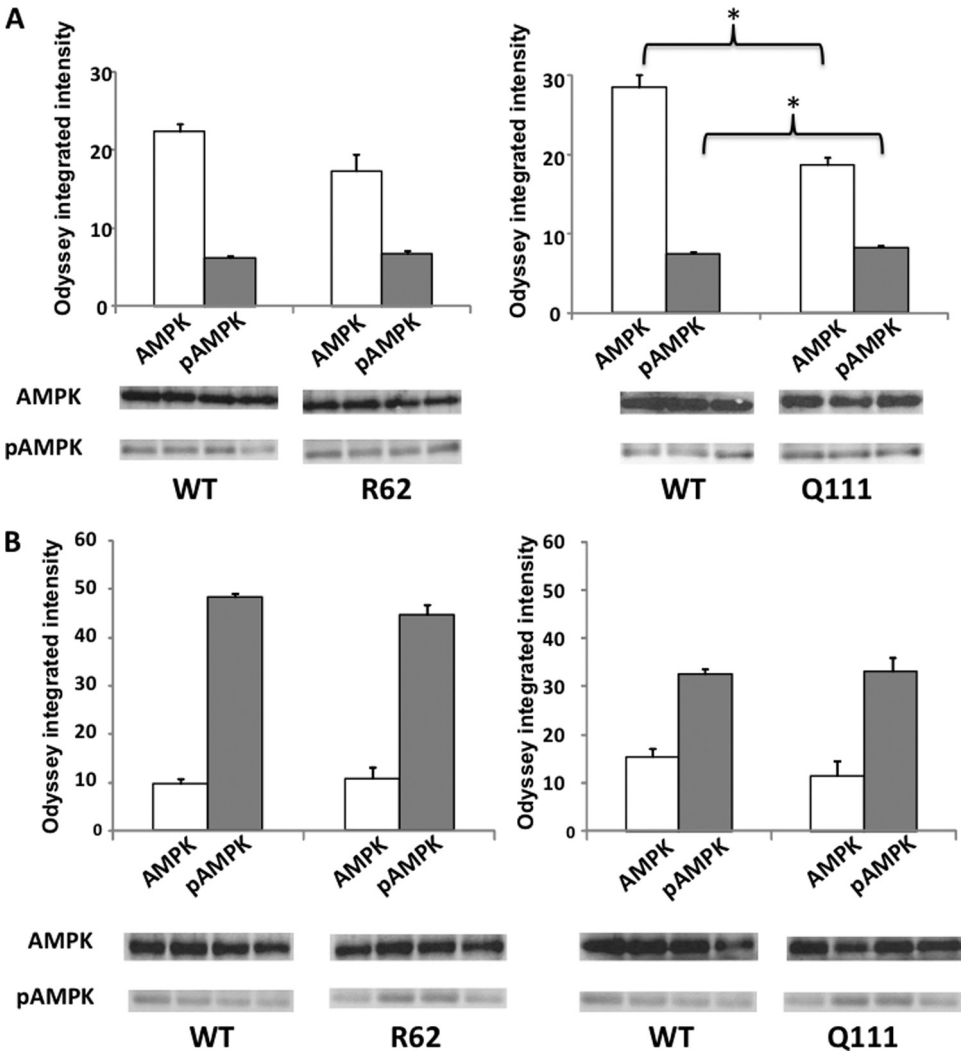

FIGURE 4. **Quantitative immunoblots of AMPK and pAMPK in R6/2 and $Hdh^{Q111/+}$ mice.** Total (AMPK) and pAMPK levels were quantified by immunoblot analyses of striatum (*A*) and frontal cortex (*B*) of 8-week-old R6/2 mice and 4-month-old $Hdh^{Q111/+}$ mice compared with WT littermates; there were four animals per group. Microwave fixation sacrifice was used to preserve steady-state phosphorylation. Representative immunoblots for AMPK and pAMPK are shown. The values represent arbitrary intensity units ± S.E. *, $p < 0.05$.

Increased pAMPK/AMPK Ratio in the Brain of R6/2 and $Hdh^{Q111/+}$ Mice—To assess the cellular energy homeostasis in HD, we measured the protein expression of AMPK and pAMPK in brain samples from R6/2 and $Hdh^{Q111/+}$ mice obtained after microwave fixation. We measured the pAMPK to AMPK ratio to normalize the specific phosphorylation state of AMPK to the total kinase protein and therefore assess signaling through the phospho-site on AMPK. Despite the absence of significant changes in AMPK and pAMPK (Fig. 4*A*), we observed an elevated pAMPK/AMPK ratio in the striatum of 8-week-old R6/2 mice compared with WT littermates ($p = 0.017$). In the striatum of 4-month-old $Hdh^{Q111/+}$ mice, we found increased expression of pAMPK (Fig. 4*A*, $p = 0.030$) and decreased expression of AMPK (Fig. 4, $p = 0.011$) compared with WT littermates, resulting in an increased pAMPK/AMPK ratio ($p = 0.003$). The protein levels of AMPK and pAMPK measured in the frontal cortex were not significantly different between WT and 4-month-old $Hdh^{Q111/+}$ mice (Fig. 4*B*). However, we found an elevated pAMPK/AMPK ratio in the frontal cortex of 4-month-old $Hdh^{Q111/+}$ mice ($p = 0.042$). The same experiments were performed on nonmicrowaved brain samples. Although the changes in AMPK expression were comparable with the ones observed in microwaved samples from R6/2 and $Hdh^{Q111/+}$ mice compared with WT littermates, we did not find any consistent changes in pAMPK expression. This result is likely due to immediate post-mortem changes as reported previously (11). Taken together, these data pinpoint altered brain cellular energy homeostasis early in the pathogenic process of HD, suggesting that brain energy deficit may also occur at presymptomatic stages in individuals with *HTT* CAG expansion alleles.

DISCUSSION

In this study, we demonstrated early alterations of brain energy homeostasis in two mouse models of HD prior to motor disease onset. We found decreased ATP levels and ATP/AMP ratio in the striatum and frontal cortex of transgenic R6/2 mice, as well as activation of AMPK, in the context of a systemic hypercatabolic state. Unexpectedly, this energy deficit was associated with an increase of the high energy phosphate phos-

Downloaded from www.jbc.org at CDC Information Center, on February 10, 2012

phocreatine and creatine in the same brain regions, resulting in an increased phosphocreatine to ATP ratio. Of note, the increase in phosphocreatine preceded both the decrease in ATP and the behavioral phenotypes that were measured in this study. Notably, striatal ATP and phosphocreatine levels were inversely correlated with the number of CAG repeats, as shown for ATP in lymphoblastoid cells of HD patients (26), indicating an important link between the brain energy deficit in the basal ganglia and the most prominent modifier of HD phenotypic expression and severity (27). Moreover, in heterozygous $Hdh^{Q111/+}$ knock-in mice, we found that the earliest metabolic changes consisted of increased phosphocreatine in the frontal cortex and increased pAMPK/AMPK ratio in both striatum and frontal cortex.

Although an energy deficit was suspected to be a response to the *HTT* CAG repeat expansion in striatum, for example based on the finding of reduced ATP levels in immortalized HD striatal neuronal cell lines (13), ATP depletion was never demonstrated directly in brain tissues of HD mouse models. Because of the immediate increase of glycolytic rates following brain death (10), the only approach that seems to circumvent post-mortem metabolic distortion is the instantaneous inactivation of brain enzymatic activities through the use of microwave irradiation. Commonly used methods of sacrifice, such as decapitation, even led to increased brain ATP levels in a rodent HD model (28). By contrast, we found decreased striatal ATP in R6/2 mice at 8 and 12 weeks of age. This finding was also evident in extrastriatal regions such as the frontal cortex, underlying the involvement of corticostriatal pathways in the pathophysiology of HD (29). Because of its key role in regulating cellular energy metabolism, the use of microwave fixation additionally allowed to accurately assess the activation of AMPK, as reflected by the pAMPK/AMPK ratio. This revealed an elevated pAMPK/AMPK ratio in the striatum and/or the frontal cortex of R6/2 and $Hdh^{Q111/+}$ mice, further emphasizing altered energy homeostasis at the earliest stages of HD. At the systemic level, we also found a hypercatabolic status in R6/2 mice, defined by decreased body weight compared with WT littermates despite early increased food intake. This confirmed earlier findings of increased metabolism reflected by increased oxygen consumption in R6/2 mice (15). In our study, the number of CAG repeats correlated with feeding behaviors, suggesting an association between hypercatabolism and disease severity, as also shown in HD patients at an early stage of the disease and in presymptomatic individuals (16). The observation that numerous protein interactors of huntingtin are involved in cellular energy metabolism (30) would warrant further studies to decipher the molecular mechanisms underlying the early energy deficit evidenced here in HD, both at the central and systemic level, in particular to assess whether a direct link between the HD mutation and the changes in energy homeostasis can be established.

Thanks to the use of noninvasive behavioral recording techniques, we confirmed that R6/2 mice sacrificed at 4 weeks of age are at a premotor stage of the disease (15, 31, 32). Therefore, it was remarkable that increased phosphocreatine and creatine levels were detected in 4-week-old R6/2 mice, preceding the decrease of ATP. Similarly, increased phosphocreatine was the earliest metabolic change that we observed in the frontal cortex of 4-month-old $Hdh^{Q111/+}$ mice. In behavioral analyses conduced in this line to date, this time point precedes a motor learning abnormality observed at 6 months of age. Previous work in which brain tissues were obtained after decapitation showed on the other hand decreased brain creatine levels in 8-week-old R6/2 mice (33). This observation encouraged the initiation of several trials of creatine supplementation in HD mouse models (33–36) despite a lack of overt benefit in HD patients so far (37, 38). However, high resolution 9.4T ^{1}H NMR spectroscopy challenged these findings by showing significantly increased creatine *in vivo* at 8 and 12 weeks in R6/2 mouse brain together with significantly increased phosphocreatine at 12 weeks (39). More recently, creatine and phosphocreatine were found to be increased but without changes in ATP levels in whole brain extracts from R6/2 and $Hdh^{Q111/+}$ mice (40). However, both mouse models were studied at late stages of the disease, and brain samples were obtained after decapitation rather than using microwave fixation.

Our observation with 3NP, an acute model of striatal degeneration, further emphasizes the relevance of our findings of an early increase of phosphocreatine and creatine in the brain of HD mice. Indeed, the decreased ATP in striatum following 3NP injection was associated with significantly decreased ADP and phosphocreatine, reflecting an acute depletion of the pool of high energy phosphates. On the contrary, in both R6/2 and $Hdh^{Q111/+}$ mice, brain energy deficit is part of a chronic neurodegenerative process in which regulatory mechanisms of cellular energy homeostasis may be altered. Likewise, the increased phosphocreatine and/or creatine in the context of normal or decreased expression of AGAT, GAMT, and SLC6A8 emphasizes that the expanded pool of the high energy phosphate phosphocreatine is likely not due to increased creatine synthesis or transport. Similar observations were reported in a chronic model of myocardial energy deficit in transgenic mice lacking expression of the glucose transport protein GLUT4. GLUT4-deficient mice exhibited increased cardiac phosphocreatine to ATP ratio because of increased creatine and phosphocreatine contents in myocytes (41), unlike models of acute myocardial energy failure, such as ischemia, that are characterized by a decreased phosphocreatine to ATP ratio.

Overall, the increased cellular pool of phosphocreatine and/or creatine in the context of AMPK activation suggests that phosphocreatine is insufficiently utilized by BB-CK for energy homeostasis. However, it is unlikely that the decrease of BB-CK that we observed early in the brain of HD mice and that previous studies reported in *HTT* transgenic mice and HD patients (42, 43) is sufficient to produce accumulation of phosphocreatine. When blocking the activity of both cytosolic and mitochondrial CK in skeletal muscle, the levels of phosphocreatine were only minimally affected but phosphocreatine could no longer serve to regenerate hydrolyzed ATP (44). Similarly, mice lacking BB-CK isoenzyme have normal brain levels of high energy metabolites and tissue pH as detected *in vivo* using ^{1}H and ^{31}P NMR spectroscopy (45). It is possible that the total content of high energy phosphates may not reflect their distribution in subcellular compartments (46). In conclusion, our data strongly suggest early alterations in homeostasis of high

Downloaded from www.jbc.org at CDC Information Center, on February 10, 2012

energy phosphates in HD, identifying that the utilization of the phosphocreatine pool might be reduced in the HD brain.

Acknowledgments—We thank Vikrant Nobla for technical assistance with the HomeCage video tracking system, Charles Scouten for input on the microwave fixation system, Teodoro Bottiglieri and Erland Arning for technical assistance with the HPLC measurements, Olivier Braissant for providing us with the AGAT and GAMT antibodies, Jolene Guide and Jason St. Claire for animal husbandry and genotyping, Brenda Billig for performing and analyzing immunoblots on microwaved samples, Cristovao Sousa for performing the RNA extraction, Derek Blankenship for statistical support, and Emile Van Schaftingen and Robert A. Harris for helpful discussion on the data.

REFERENCES

1. Gusella, J. F., Wexler, N. S., Conneally, P. M., Naylor, S. L., Anderson, M. A., Tanzi, R. E., Watkins, P. C., Ottina, K., Wallace, M. R., and Sakaguchi, A. Y. (1983) A polymorphic DNA marker genetically linked to Huntington's disease. *Nature* **306,** 234–238
2. The Huntington's Disease Collaborative Research Group (1993) A novel gene containing a trinucleotide repeat that is expanded and unstable on Huntington's disease chromosomes. *Cell* **72,** 971–983
3. Ciarmiello, A., Cannella, M., Lastoria, S., Simonelli, M., Frati, L., Rubinsztein, D. C., and Squitieri, F. (2006) Brain white-matter volume loss and glucose hypometabolism precede the clinical symptoms of Huntington's disease. *J. Nucl. Med.* **47,** 215–222
4. Mochel, F., and Haller, R. G. (2011) Energy deficit in Huntington disease: why it matters. *J. Clin. Invest.* **121,** 493–499
5. Milakovic, T., and Johnson, G. V. (2005) Mitochondrial respiration and ATP production are significantly impaired in striatal cells expressing mutant huntingtin. *J. Biol. Chem.* **280,** 30773–30782
6. Powers, W. J., Videen, T. O., Markham, J., McGee-Minnich, L., Antenor-Dorsey, J. V., Hershey, T., and Perlmutter, J. S. (2007) Selective defect of *in vivo* glycolysis in early Huntington's disease striatum. *Proc. Natl. Acad. Sci. U.S.A.* **104,** 2945–2949
7. Cui, L., Jeong, H., Borovecki, F., Parkhurst, C. N., Tanese, N., and Krainc, D. (2006) Transcriptional repression of PGC-1α by mutant huntingtin leads to mitochondrial dysfunction and neurodegeneration. *Cell* **127,** 59–69
8. Beal, M. F. (1994) Neurochemistry and toxin models in Huntington's disease. *Curr. Opin. Neurol.* **7,** 542–547
9. Brouillet, E., Jacquard, C., Bizat, N., and Blum, D. (2005) 3-Nitropropionic acid: a mitochondrial toxin to uncover physiopathological mechanisms underlying striatal degeneration in Huntington's disease. *J. Neurochem.* **95,** 1521–1540
10. Lowry, O. H., Passonneau, J. V., Hasselberger, F. X., and Schulz, D. W. (1964) Effect of ischemia on known substrates and cofactors of the glycolytic pathway in brain. *J. Biol. Chem.* **239,** 18–30
11. Scharf, M. T., Mackiewicz, M., Naidoo, N., O'Callaghan, J. P., and Pack, A. I. (2008) AMP-activated protein kinase phosphorylation in brain is dependent on method of killing and tissue preparation. *J. Neurochem.* **105,** 833–841
12. Delaney, S. M., and Geiger, J. D. (1996) Brain regional levels of adenosine and adenosine nucleotides in rats killed by high-energy focused microwave irradiation. *J. Neurosci. Methods* **64,** 151–156
13. Gines, S., Seong, I. S., Fossale, E., Ivanova, E., Trettel, F., Gusella, J. F., Wheeler, V. C., Persichetti, F., and MacDonald, M. E. (2003) Specific progressive cAMP reduction implicates energy deficit in presymptomatic Huntington's disease knock-in mice. *Hum. Mol. Genet.* **12,** 497–508
14. Weydt, P., Pineda, V. V., Torrence, A. E., Libby, R. T., Satterfield, T. F., Lazarowski, E. R., Gilbert, M. L., Morton, G. J., Bammler, T. K., Strand, A. D., Cui, L., Beyer, R. P., Easley, C. N., Smith, A. C., Krainc, D., Luquet, S., Sweet, I. R., Schwartz, M. W., and La Spada, A. R. (2006) Thermoregulatory and metabolic defects in Huntington's disease transgenic mice implicate PGC-1α in Huntington's disease neurodegeneration. *Cell Metab.* **4,** 349–362
15. van der Burg, J. M., Bacos, K., Wood, N. I., Lindqvist, A., Wierup, N., Woodman, B., Wamsteeker, J. I., Smith, R., Deierborg, T., Kuhar, M. J., Bates, G. P., Mulder, H., Erlanson-Albertsson, C., Morton, A. J., Brundin, P., Petersén, A., and Björkqvist, M. (2008) Increased metabolism in the R6/2 mouse model of Huntington's disease. *Neurobiol. Dis.* **29,** 41–51
16. Mochel, F., Charles, P., Seguin, F., Barritault, J., Coussieu, C., Perin, L., Le Bouc, Y., Gervais, C., Carcelain, G., Vassault, A., Feingold, J., Rabier, D., and Durr, A. (2007) Early energy deficit in Huntington disease: identification of a plasma biomarker traceable during disease progression. *PLoS One* **2,** e647
17. Wheeler, V. C., Auerbach, W., White, J. K., Srinidhi, J., Auerbach, A., Ryan, A., Duyao, M. P., Vrbanac, V., Weaver, M., Gusella, J. F., Joyner, A. L., and MacDonald, M. E. (1999) Length-dependent gametic CAG repeat instability in the Huntington's disease knock-in mouse. *Hum. Mol. Genet.* **8,** 115–122
18. Lee, J. M., Pinto, R. M., Gillis, T., St Claire, J. C., and Wheeler, V. C. (2011) Quantification of age-dependent somatic CAG repeat instability in Hdh CAG knock-in mice reveals different expansion dynamics in striatum and liver. *PLoS One* **6,** e23647
19. Dragileva, E., Hendricks, A., Teed, A., Gillis, T., Lopez, E. T., Friedberg, E. C., Kucherlapati, R., Edelmann, W., Lunetta, K. L., MacDonald, M. E., and Wheeler, V. C. (2009) Intergenerational and striatal CAG repeat instability in Huntington's disease knock-in mice involve different DNA repair genes. *Neurobiol. Dis.* **33,** 37–47
20. O'Callaghan, J. P., and Sriram, K. (2004) Focused microwave irradiation of the brain preserves in vivo protein phosphorylation: comparison with other methods of sacrifice and analysis of multiple phosphoproteins. *J. Neurosci. Methods* **135,** 159–168
21. Williams, J. H., Vidt, S. E., and Rinehart, J. (2008) Measurement of sarcoplasmic reticulum Ca^{2+} ATPase activity using high-performance liquid chromatography. *Anal. Biochem.* **372,** 135–139
22. Braissant, O., Henry, H., Villard, A. M., Speer, O., Wallimann, T., and Bachmann, C. (2005) Creatine synthesis and transport during rat embryogenesis: spatiotemporal expression of AGAT, GAMT and CT1. *BMC Dev. Biol.* **5,** 9
23. Smith, P. K., Krohn, R. I., Hermanson, G. T., Mallia, A. K., Gartner, F. H., Provenzano, M. D., Fujimoto, E. K., Goeke, N. M., Olson, B. J., and Klenk, D. C. (1985) Measurement of protein using bicinchoninic acid. *Anal. Biochem.* **150,** 76–85
24. Morton, A. J., Glynn, D., Leavens, W., Zheng, Z., Faull, R. L., Skepper, J. N., and Wight, J. M. (2009) Paradoxical delay in the onset of disease caused by super-long CAG repeat expansions in R6/2 mice. *Neurobiol. Dis.* **33,** 331–341
25. Chan, P., DeLanney, L. E., Irwin, I., Langston, J. W., and Di Monte, D. (1991) Rapid ATP loss caused by 1-methyl-4-phenyl-1,2,3,6-tetrahydropyridine in mouse brain. *J. Neurochem.* **57,** 348–351
26. Seong, I. S., Ivanova, E., Lee, J. M., Choo, Y. S., Fossale, E., Anderson, M., Gusella, J. F., Laramie, J. M., Myers, R. H., Lesort, M., and MacDonald, M. E. (2005) HD CAG repeat implicates a dominant property of huntingtin in mitochondrial energy metabolism. *Hum. Mol. Genet.* **14,** 2871–2880
27. Snell, R. G., MacMillan, J. C., Cheadle, J. P., Fenton, I., Lazarou, L. P., Davies, P., MacDonald, M. E., Gusella, J. F., Harper, P. S., and Shaw, D. J. (1993) Relationship between trinucleotide repeat expansion and phenotypic variation in Huntington's disease. *Nat. Genet.* **4,** 393–397
28. Oláh, J., Klivényi, P., Gardián, G., Vécsei, L., Orosz, F., Kovacs, G. G., Westerhoff, H. V., and Ovádi, J. (2008) Increased glucose metabolism and ATP level in brain tissue of Huntington's disease transgenic mice. *FEBS J.* **275,** 4740–4755
29. Thu, D. C., Oorschot, D. E., Tippett, L. J., Nana, A. L., Hogg, V. M., Synek, B. J., Luthi-Carter, R., Waldvogel, H. J., and Faull, R. L. (2010) Cell loss in the motor and cingulate cortex correlates with symptomatology in Huntington's disease. *Brain* **133,** 1094–1110
30. Kaltenbach, L. S., Romero, E., Becklin, R. R., Chettier, R., Bell, R., Phansalkar, A., Strand, A., Torcassi, C., Savage, J., Hurlburt, A., Cha, G. H., Ukani, L., Chepanoske, C. L., Zhen, Y., Sahasrabudhe, S., Olson, J., Kurschner, C., Ellerby, L. M., Peltier, J. M., Botas, J., and Hughes, R. E. (2007) Huntingtin interacting proteins are genetic modifiers of neurodegenera-

Downloaded from www.jbc.org at CDC Information Center, on February 10, 2012

tion. *PLoS Genet.* **3,** e82
31. Steele, A. D., Jackson, W. S., King, O. D., and Lindquist, S. (2007) The power of automated high-resolution behavior analysis revealed by its application to mouse models of Huntington's and prion diseases. *Proc. Natl. Acad. Sci. U.S.A.* **104,** 1983–1988
32. Rudenko, O., Tkach, V., Berezin, V., and Bock, E. (2009) Detection of early behavioral markers of Huntington's disease in R6/2 mice employing an automated social home cage. *Behav. Brain Res.* **203,** 188–199
33. Dedeoglu, A., Kubilus, J. K., Yang, L., Ferrante, K. L., Hersch, S. M., Beal, M. F., and Ferrante, R. J. (2003) Creatine therapy provides neuroprotection after onset of clinical symptoms in Huntington's disease transgenic mice. *J. Neurochem.* **85,** 1359–1367
34. Ferrante, R. J., Andreassen, O. A., Jenkins, B. G., Dedeoglu, A., Kuemmerle, S., Kubilus, J. K., Kaddurah-Daouk, R., Hersch, S. M., and Beal, M. F. (2000) Neuroprotective effects of creatine in a transgenic mouse model of Huntington's disease. *J. Neurosci.* **20,** 4389–4397
35. Andreassen, O. A., Jenkins, B. G., Dedeoglu, A., Ferrante, K. L., Bogdanov, M. B., Kaddurah-Daouk, R., and Beal, M. F. (2001) Increases in cortical glutamate concentrations in transgenic amyotrophic lateral sclerosis mice are attenuated by creatine supplementation. *J. Neurochem.* **77,** 383–390
36. Yang, L., Calingasan, N. Y., Wille, E. J., Cormier, K., Smith, K., Ferrante, R. J., and Beal, M. F. (2009) Combination therapy with coenzyme Q10 and creatine produces additive neuroprotective effects in models of Parkinson's and Huntington's diseases. *J. Neurochem.* **109,** 1427–1439
37. Verbessem, P., Lemiere, J., Eijnde, B. O., Swinnen, S., Vanhees, L., Van Leemputte, M., Hespel, P., and Dom, R. (2003) Creatine supplementation in Huntington's disease: a placebo-controlled pilot trial. *Neurology* **61,** 925–930
38. Tabrizi, S. J., Blamire, A. M., Manners, D. N., Rajagopalan, B., Styles, P., Schapira, A. H., and Warner, T. T. (2005) High-dose creatine therapy for Huntington disease: a 2-year clinical and MRS study. *Neurology* **64,** 1655–1656
39. Tkac, I., Dubinsky, J. M., Keene, C. D., Gruetter, R., and Low, W. C. (2007) Neurochemical changes in Huntington R6/2 mouse striatum detected by *in vivo* 1H NMR spectroscopy. *J. Neurochem.* **100,** 1397–1406
40. Zhang, S. F., Hennessey, T., Yang, L., Starkova, N. N., Beal, M. F., and Starkov, A. A. (2011) Impaired brain creatine kinase activity in Huntington's disease. *Neurodegener. Dis.* **8,** 194–201
41. Weiss, R. G., Chatham, J. C., Georgakopolous, D., Charron, M. J., Wallimann, T., Kay, L., Walzel, B., Wang, Y., Kass, D. A., Gerstenblith, G., and Chacko, V. P. (2002) An increase in the myocardial PCr/ATP ratio in GLUT4 null mice. *FASEB J.* **16,** 613–615
42. Kim, J., Amante, D. J., Moody, J. P., Edgerly, C. K., Bordiuk, O. L., Smith, K., Matson, S. A., Matson, W. R., Scherzer, C. R., Rosas, H. D., Hersch, S. M., and Ferrante, R. J. (2010) Reduced creatine kinase as a central and peripheral biomarker in Huntington's disease. *Biochim. Biophys. Acta* **1802,** 673–681
43. Lin, Y. S., Chen, C. M., Soong, B. W., Wu, Y. R., Chen, H. M., Yeh, W. Y., Wu, D. R., Lin, Y. J., Poon, P. W., Cheng, M. L., Wang, C. H., and Chern, Y. (2011) Dysregulated brain creatine kinase is associated with hearing impairment in mouse models of Huntington disease. *J. Clin. Invest.* **121,** 1519–1523
44. Steeghs, K., Benders, A., Oerlemans, F., de Haan, A., Heerschap, A., Ruitenbeek, W., Jost, C., van Deursen, J., Perryman, B., Pette, D., Brückwilder, M., Koudijs, J., Jap, P., Veerkamp, J., and Wieringa, B. (1997) Altered Ca^{2+} responses in muscles with combined mitochondrial and cytosolic creatine kinase deficiencies. *Cell* **89,** 93–103
45. in 't Zandt, H. J., Renema, W. K., Streijger, F., Jost, C., Klomp, D. W., Oerlemans, F., Van der Zee, C. E., Wieringa, B., and Heerschap, A. (2004) Cerebral creatine kinase deficiency influences metabolite levels and morphology in the mouse brain: a quantitative *in vivo* 1H and 31P magnetic resonance study. *J. Neurochem.* **90,** 1321–1330
46. Saks, V., Dos Santos, P., Gellerich, F. N., and Diolez, P. (1998) Quantitative studies of enzyme-substrate compartmentation, functional coupling and metabolic channelling in muscle cells. *Mol. Cell Biochem.* **184,** 291–307
47. Matthews, R. T., Yang, L., Jenkins, B. G., Ferrante, R. J., Rosen, B. R., Kaddurah-Daouk, R., and Beal, M. F. (1998) *J. Neurosci.* **18,** 156–163

Downloaded from www.jbc.org at CDC Information Center, on February 10, 2012